Irradiation Test of 65-nm Bulk SRAMs With DC Muon Beam at RCNP-MuSIC Facility

Takumi Mahara, Seiya Manabe, Yukinobu Watanabe, Wang Liao, Masanori Hashimoto, Takeshi Y. Saito, Megumi Niikura, Kazuhiko Ninomiya, Dai Tomono, and Akira Sato

***Abstract*— Negative and positive muon irradiation tests of static random access memories (SRAMs) were performed at Muon Science Innovation Channel (MuSIC) of Research Center for Nuclear Physics (RCNP), Osaka University. The muon-induced single event upset (SEU) cross sections for 65-nm bulk SRAMs were measured. The SRAM device was irradiated by the muon beams with average momenta ranging from 37.8 to 41.0 MeV/c at the beam exit. The incident muon fluence was measured using a one-by-one muon detection system with a plastic scintillator by taking advantage of the direct current (dc) muon beam and reliable absolute values of SEU cross sections were obtained. In addition to the measurement of the SEU cross sections, we measured muonic X-rays from the irradiated device to investigate the relation between the measured SEU cross section and the emission rate of muonic X-rays associated with the stopping position of the muons as a function of incident muon momentum. The result suggested that negative muons have a significant effect on SEUs by the emission of secondary light ions via negative muon capture reaction when negative muons stop near sensitive volumes (SVs) in SRAMs.**

***Index Terms*— 65-nm bulk static random access memory (SRAM), irradiation test, muonic X-rays, negative positive muons, Research Center for Nuclear Physics-Muon Science Innovation Channel (RCNP-MuSIC), single event upset (SEU).**

Manuscript received October 8, 2019; revised November 17, 2019; accepted December 17, 2019. Date of publication February 6, 2020; date of current version July 16, 2020. This work was supported in part by JSPS KAKENHI under Grant JP16H03906 and in part by JST-OPERA Program, Japan, under Grant JPMJOP1721.

Takumi Mahara, Seiya Manabe, and Yukinobu Watanabe are with the Department of Advanced Energy Engineering Science, Kyushu University, Fukuoka 816-8580, Japan (e-mail: mahara.takumi.308@s.kyushu-u.ac.jp; manabe@aees.kyushu-u.ac.jp; watanabe@aees.kyushu-u.ac.jp).

Wang Liao was with the Department of Information System Engineering, Osaka University, Suita 565-0871, Japan. He is now with the School of Systems Engineering, Kochi University of Technology, Kami 782-8502, Japan (e-mail: liao.wang@kochi-tech.ac.jp).

Masanori Hashimoto is with the Department of Information Systems Engineering, Osaka University, Suita 565-0871, Japan (e-mail: hasimoto@ist.osaka-u.ac.jp).

Takeshi Y. Saito and Megumi Niikura are with the Department of Physics, The University of Tokyo, Tokyo 113-0033, Japan (e-mail: saito@nex.phys.s.u-tokyo.ac.jp; niikura@nex.phys.s.u-tokyo.ac.jp).

Kazuhiko Ninomiya is with the Graduate School of Science, Osaka University, Toyonaka 560-0043, Japan (e-mail: ninokazu@chem.sci.osaka-u.ac.jp).

Dai Tomono is with the Research Center for Nuclear Physics (RCNP), Osaka University, Ibaraki 567-0047, Japan (e-mail: tomono@rcnp.osaka-u.ac.jp).

Akira Sato is with the Graduate School of Science, Osaka University, Toyonaka 560-0043, Japan, and also with the Research Center for Nuclear Physics (RCNP), Osaka University, Ibaraki 567-0047, Japan (e-mail: sato@phys.sci.osaka-u.ac.jp).

Color versions of one or more of the figures in this article are available online at http://ieeexplore.ieee.org.

Digital Object Identifier 10.1109/TNS.2020.2972022

I. Introduction

RADIATION-INDUCED soft error means a temporary fault in very large scale integrated (VLSI) circuits due to single event upset (SEU), i.e., upset of memory information in a static random access memory (SRAM). On the ground, a main cause of the soft error has so far been recognized as neutrons among the species of secondary cosmic-rays. Recently, muon-induced soft errors are drawing attention due to the reduction of soft error immunity on SRAMs, and many works have been devoted to investigate the effect of cosmic-ray muons on the occurrence of SEUs [1]–[12]. From previous experimental and simulation works [7]–[12], it was found that negative muons cause SEUs more significantly compared to positive muons because of the effect of negative muon capture reactions [13]. In [11], the muon SEU rates at ground level for the 65-nm SRAMs [8]–[10] were estimated based on the experimental SEU cross section data and compared with the neutron SEU rates of the same SRAMs. The result showed that the muon SEU rates are 0.1–1% of the neutron SEU rates. However, the relative proportion of the muon SEU rate to the neutron SEU rate was found to increase up to about 10% on the first floor of a five-story building because of the relatively large attenuation of neutron flux and less attenuation of muon flux in the building. In addition, a muon irradiation test [12] for 28-nm SRAMs revealed that the muon SEU cross section increases and the neutron SEU cross section decreases according to the technology advancement [14]. These recent works on muon-induced SEUs suggest a need for further study to enhance the understanding of the SEU mechanism.

In this article, the irradiation test for 65-nm bulk and ultra-thin body and thin buried oxide silicon-on-insulator SRAMs was performed to measure the negative and positive muon SEU cross sections [8], [9]. The SEU experiment was conducted at the muon science facility (MUSE) [15], [16] in Materials and Life Science Experimental Facility of the Japan Proton Accelerator Research Complex (J-PARC). The SEU cross sections were obtained as the ratio of the number of bit errors to incident muon fluence. The pulsed muon beam with a repetition rate of 25 Hz is available at MUSE. Approximately 10^4 muons were bunched in a pulse with about 100-ns width during the experiment. The muon fluence was indirectly measured by counting the number of decay electrons/positrons that were emitted from stopped muons. Hence, there is an uncertainty in the measurement of the muon fluence. In this article, we performed a new experiment with

a direct current (dc) muon beam at Muon Science Innovation Channel (MuSIC) [17] in Research Center for Nuclear Physics (RCNP), Osaka University, in order to make the measured cross section more reliable. The MuSIC beamline provides the muon beam with a continuous time structure with an intensity of approximately 2×10^3 muons/s. Therefore, a single muon can be detected individually and reliable absolute values of SEU cross sections can be obtained.

In addition to the SEU cross section measurement, we conducted a muonic X-ray measurement. When the negative muon stops in matter, it is captured by a nucleus at high orbital momentum state of the muonic atom. The captured negative muon cascades down to a 1-s orbital while emitting muonic X-rays. The energy of the muonic X-ray is unique to the atomic number of the captured element. Hence, the elements existing in the stopping position of the negative muon can be identified by the muonic X-ray energy in a nondestructive way [18]. Besides, our previous experimental results [8], [9] pointed out that the negative muon has a significant effect on the occurrence of SEUs when the muon stopped near the sensitive volumes (SVs) and it emits secondary light ions (protons, deuterons, α particles, etc.) via the capture reaction. Therefore, information on the muon stopping position and the constituent elements at its position is important to study the mechanisms of SEUs induced by negative muons. Thus, we have performed a preliminary measurement of the muonic X-rays to see the feasibility of element identification at the muon stopping position.

II. Experiment

A. Test Facility

The accelerated test with negative and positive muons was performed using RCNP-MuSIC [17]. The muons are decay products of pions. The facility produces the pions through nuclear reactions between a 392-MeV proton beam and a 20-cm-thick graphite cylindrical target. The produced pions are collected by using a capture solenoid and they are guided into the beamline where they decay subsequently to the muons. The 392-MeV proton cyclotron was operated with an average current of 1.1 μA during the test. The momentum distribution of the muon beam was measured as a normal distribution with an approximately 7.0% standard deviation at the beam exit using a time of flight method. The incident muon fluence can be measured directly, thanks to the dc muon beam.

B. Experimental Setup

The test SRAM chips were fabricated in 65-nm bulk CMOS technology with a deep well option. Fig. 1 shows the device board under test. Sixteen SRAM chips are mounted on a piece of printed circuit board (PCB). Each chip has 12-Mb memories. The same test board was used in the previous muon experiment at the MUSE facility and the details of the device board are described in [9].

The experimental setup is schematically illustrated in Fig. 2. The setup was constructed at the downstream of the beam exit. The beam exit was equipped with a 75-μm-thick Kapton film to seal a vacuum of the beamline. The reverse side

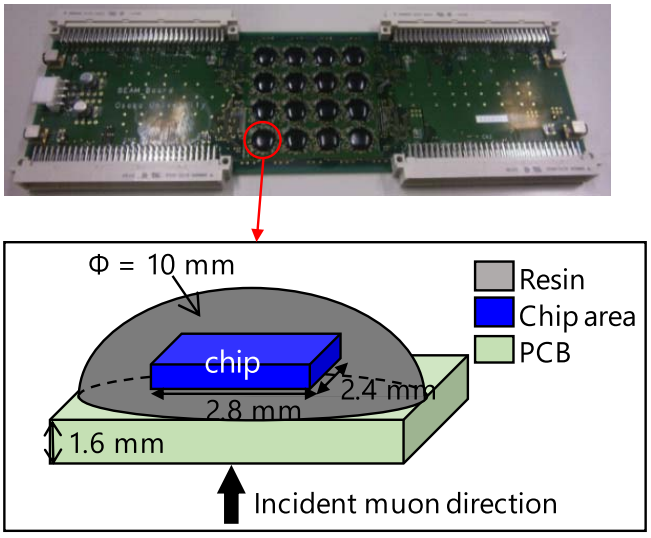

Fig. 1. Structure of the device board. Sixteen chips are bonded on the 1.6-mm-thick PCB. The thickness of tested chips is approximately 0.3 mm.

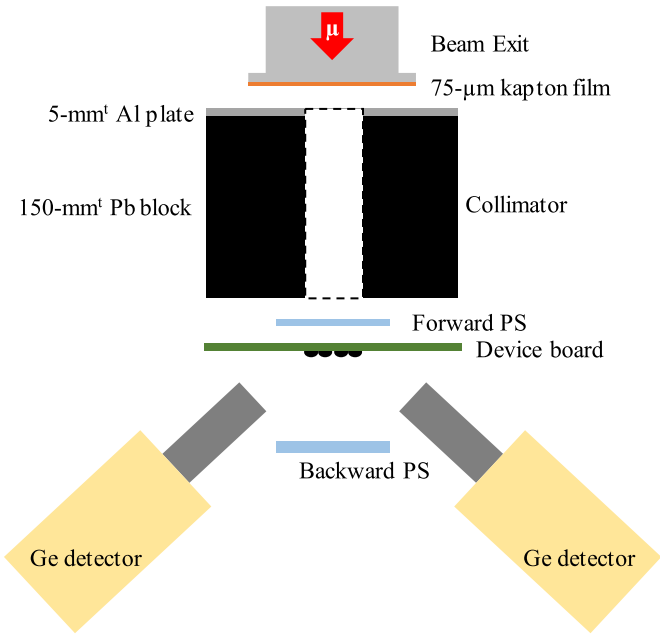

Fig. 2. Schematic experimental setup for muon irradiation at MuSIC facility.

of the device board was irradiated with the muon beam passing through the collimator. The collimator consisted of a 5-mm-thick aluminum plate and piled-up 150-mm-thick lead blocks. The collimator slit was 55 mm $\times$ 55 mm squared-shaped. Sixteen chips, i.e., 192-Mb SRAMs in the device board were irradiated. In front of the device board, a plastic scintillator (PS) was placed to measure the muon incident fluence. The size of the forward PS was 100 mm $\times$ 100 mm and the thickness was 0.4 mm. Another PS with a size of 100 mm $\times$ 100 mm $\times$ 5 mm thickness was placed at the downstream of the board. The backward PS detected muons passed through the device board. The negative and positive muon-induced SEU cross sections were derived by dividing the number of bit errors by the product of the incident muon fluence and the total number of irradiated bits, i.e., 192 Mb.

To measure the SEU cross sections, we first conducted momentum scanning with the negative muon beam for the SRAM chips operating at the voltage of 0.9 V. The aim of the momentum scanning is to search the maximum value of the SEU cross section. Next, the operating voltage was set to be 0.5 and 0.4 V, and both negative and positive muons were irradiated to observe the effect of negative muon capture reactions.

Two germanium detectors (GLP36300 and BE2020 manufactured by ORTEC and CANBERRA, respectively) were placed to detect the muonic X-rays emitted from the device board. The energy spectra of the muonic X-rays were measured during muon irradiation on the device board. The dynamic energy range of the germanium detectors was set to be about 1 MeV, which is large enough to detect 400-keV Kα muonic X-rays from silicon in the SRAM chips. The emission rate of the 400-keV Kα muonic X-rays from the device board was measured under the irradiation of negative muons with different incident momenta. Since the PCB also contains a large amount of Si as in the SRAM chips and resins, we performed an additional irradiation test on the PCB without the SRAM chips and resins in order to estimate the contribution of the muonic X-rays from Si in the PCB.

III. Experimental Results and Discussion

A. Background Run

To estimate the probability of SEUs induced by background radiations (e.g., thermal neutrons and gamma-rays), another device board was operated for monitoring. This reference board was placed under a stage on which the target device board was set. The result showed that the number of errors observed in the reference board was less than 2% of that in the irradiated device and was negligibly small. A 5-mm-thick aluminum plate was placed between the forward PS and the device board. In this case, all negative muons were completely stopped in the plate and various kinds of generated radiations other than muons (i.e., decay electrons, neutrons, gamma-rays, etc.) bombarded the device board. As a result, no SEU was observed under this situation. Thus, we confirmed that the probability of SEU induced by background radiations was negligible.

B. Incident Muon Fluence

The forward PS was used to measure the incident muon fluence. The pulse height of the analog output signal from the scintillator was converted to a digital value by an analog-to-digital converter (ADC). The ADC spectrum of the scintillator output is shown in Fig. 3. The incident beam includes electrons as contamination. The muon deposition energy is larger than the electron one. Hence, a peak of the muon is observed in the higher channel range compared to that of the electron as shown in Fig. 3. To distinguish the muon events from all the other events, the threshold channel value was set to around 700 channels where the spectrum has the minimum value between the peaks of muons and electrons, and the events over the threshold were integrated to derive the incident muon fluence. To investigate the systematic uncertainty in the derivation of the incident muon fluence, the threshold

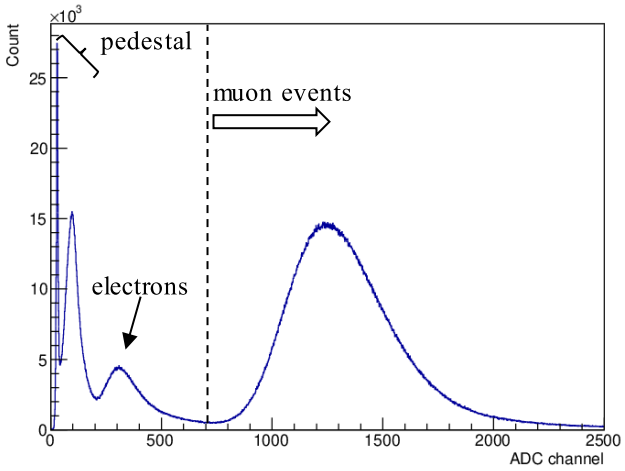

Fig. 3. ADC spectrum of the forward PS at the incident momentum of 38.9 MeV/c at beam exit.

channel was tentatively set to be 600 and 800 ch. However, the variation of the derived fluence was only 2%. As a result, the systematic error caused by the contamination of electrons in the incident muon fluence is assumed to be 2% in the present analysis.

C. SEU Cross Section

The negative muon SEU cross sections were measured as a function of incident muon momentum that is defined as the mean momentum just before the muons enter the device board. Therefore, it is different from the momentum at the beam exit because of the energy loss in the materials between the beam exit and the device board as can be seen in Fig. 2. Note that the incident momentum at the beam exit was used in the literature of our previous MUSE experiments [8], [9]. Since both experiments were performed in different irradiation configurations, the momentum just before the muons entering the device board is used for comparison of both the experimental results in this article. The momentum was estimated by the energy loss simulation with the Particle and Heavy Ion Transport code System (PHITS) [19] for both the cases, because the momentum values at the beam exit were provided from each experimental facility. Since the muon beam has a momentum distribution, the measured SEU cross section represents the averaged value over the momentum distribution $\langle\sigma_{\mathrm{SEU}}\rangle$, which is defined by the following expression:

$$\langle\sigma_{\mathrm{SEU}}(p_{\mathrm{mean}})\rangle = \frac{\int_0^\infty \sigma_{\mathrm{SEU}}(p)\cdot\phi(p,\, p_{\mathrm{mean}})dp}{\int_0^\infty \phi(p,\, p_{\mathrm{mean}})dp} \qquad (1)$$

where p_{mean} represents the mean momentum in the momentum distribution, $\sigma_{\mathrm{SEU}}(p)$ is the mono-momentum muon SEU cross section at the momentum p, and $\phi(p,\, p_{\mathrm{mean}})$ is the fluence of incident muons with the momentum p in the case of muon irradiation with the mean momentum p_{mean}. The momentum distribution can be approximated by a normal distribution with the standard deviation of 9.5% at MuSIC and 5.8% at MUSE, respectively, for the incident momentum of 35.9 MeV/c, which corresponds to 7.0% and 5.0% at the beam exit.

The measured SEU cross sections are plotted as a function of incident muon momentum and compared with the previous

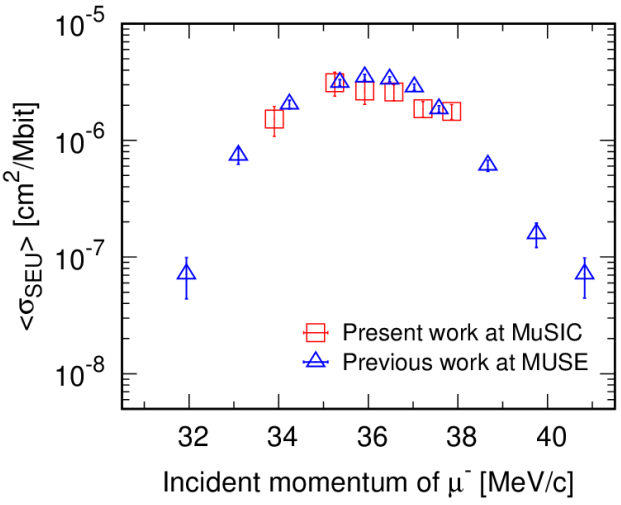

Fig. 4. Comparison of the negative muon-induced SEU cross sections measured at MuSIC and MUSE. The data at MUSE was obtained from [9] and [10]. The SRAM chips were operated at the voltage of 0.9 V.

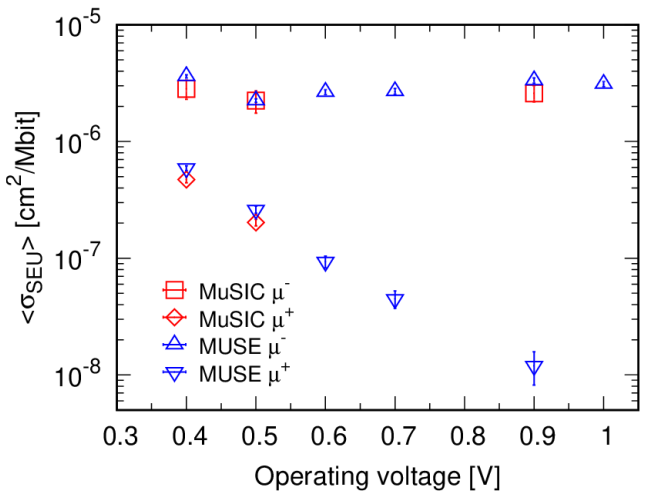

Fig. 5. Comparison of the negative and positive muon-induced SEU cross sections measured at MuSIC and MUSE. The data at MUSE was obtained from [9] and [10]. The means of momentum of muons are 36.6 MeV/c at MuSIC and 36.5 MeV/c at MUSE.

measurement with MUSE pulse beams [9] in Fig. 4. The error bars show only statistical uncertainties. There was no noticeable difference between the measured SEU cross sections at MuSIC and those at MUSE. However, the magnitude is slightly different between them. It could be partially caused by the difference in the momentum distribution between MUSE and MuSIC beams. When a muon stops near the SV, it can deposit the maximum charge because of the Bragg peak and/or the negative muon capture reaction as mentioned in [2], [7], and [8]. In the present test condition, muons with the momentum of about 36 MeV/c seem to be able to stop near the SVs because both momentum dependences of SEU cross sections in MUSE and MuSIC have peaks around 36 MeV/c. The MuSIC beam has a larger standard deviation than the MUSE beam as mentioned before. This indicates that the ratio of 36-MeV/c muons to total muons in MuSIC is smaller than that in MUSE. Thus, we believe that the momentum dependence measured in this article is in good agreement with that in the previous work.

The negative and positive muon-induced SEU cross sections for the SRAMs having the operating voltage of 0.4 and 0.5 V are shown in Fig. 5. The SRAMs operating at the voltage of 0.9 V were not irradiated by the positive muon beam because the lower error rate requires a longer test time to obtain the sufficient statistics. The voltage dependence shows good agreement with that observed in the previous work [9], as the momentum dependence does in Fig. 4. The negative-muon SEU cross-sections are about 6 and 11 times larger than the positive-muon ones in the case of 0.4- and 0.5-V operating voltages, respectively.

D. Muonic X-Rays

The measurement of muonic X-rays under irradiation can provide direct evidence that the incident muon stops in matter and is captured by a constituent atom in the stopping position. The energy spectra of the muonic X-rays were measured under the muon irradiation to both the SRAM device and PCB

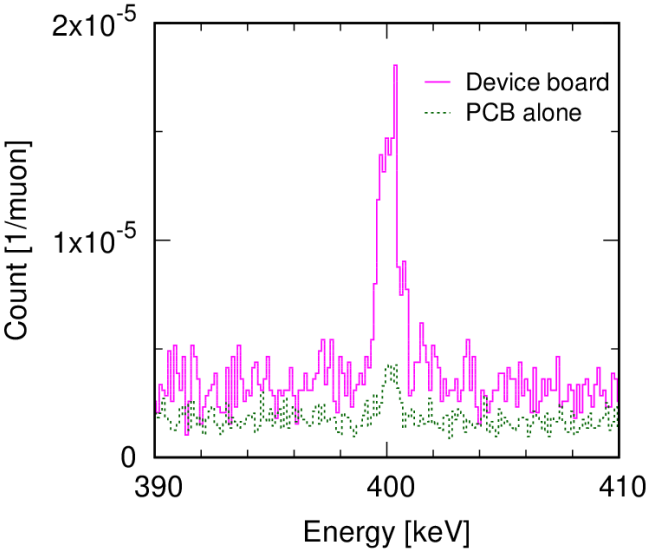

Fig. 6. Energy spectra of muonic X-rays emitted from the device board (magenta solid line) or the PCB alone (green dotted line). The incident muon incident momentum is 36.6 MeV/c, which corresponds to 39.9 MeV/c at the beam exit. The energy of silicon Kα muonic X-ray is about 400 keV.

boards. They were irradiated by the negative muon beams with the incident momentum of 33.9, 35.3, and 36.6 MeV/c, which correspond to 37.8, 38.9, and 39.9 MeV/c at the beam exit, respectively, and the emitted muonic X-rays were measured by the germanium detectors.

In the data analysis, we focused on 400-keV Kα muonic X-rays from silicon. The energy spectra measured under the irradiation of the 36.6-MeV/c muon beam for the device board and the PCB alone are shown in Fig. 6. The detection counts of the X-rays are normalized by the number of incident muons. The peaks around 400 keV are observed in both the device board and PCB. The peak counts in the PCB case are less than those in the device board case. By subtracting the former counts from the latter ones, the emission rate of silicon Kα muonic X-rays from the chip part including the chip and resin per incident muon was derived. The relation among the

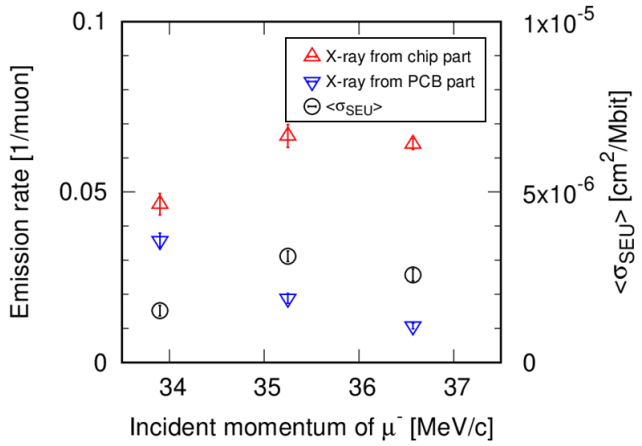

Fig. 7. Relationship between the emission rate of muonic X-rays from chips or resin and the negative muon SEU cross section. The SEU cross section was measured for the 65-nm bulk SRAMs at the operating voltage of 0.9 V.

emission rate from the chip part, the emission rate from the PCB and the negative muon SEU cross section is plotted as a function of incident muon momentum in Fig. 7. The measured emission rate of silicon Kα muonic X-rays from the chip part increases as the momentum of the incident negative muons increase while that from the PCB decreases. This trend indicates that the number of muons penetrating the PCB and reaching the chip part increases as the momentum of the incident muon increases. Furthermore, the measured emission rate of Kα muonic X-rays from the chip part shows the momentum dependence similar to that of the SEU cross sections. The intensity of the muonic X-rays is propositional to the number of stopping muons that are captured by silicon atoms in the chip part. Therefore, this experimental result suggests that the number of negative muons stopped near the SVs in SRAMs has a positive correlation with the occurrence of SEUs.

IV. Summary and Conclusion

We have conducted an irradiation test for the 65-nm bulk SRAMs with the dc muon beams at RCNP-MuSIC facility. The incident muon fluence was measured one by one using a PS by taking advantage of the dc beam with the systematic error only 2%. Thus, reliable absolute values of SEU cross sections were successfully obtained. The measured negative and positive muon SEU cross sections showed a good agreement with those measured in the MUSE facility [8], [9]. Thus, the previous MUSE result was validated by the present MuSIC result. Moreover, our present and past works demonstrated that two muon facilities in Japan are available for muon irradiation tests of memory devices.

In addition to the cross section measurement, the energy spectra of muonic X-rays were measured to investigate the muon stopping position in the irradiated device. The positive correlation between the SEU cross section and the emission rate of muonic X-rays from the SRAM chips or resins was observed. The X-ray measurement demonstrated the importance of the stopping negative muon, i.e., the negative muon capture reaction, near SVs on the occurrence of SEUs, which was suggested by the simulation in [8].

For further quantitative discussion and understanding on the mechanism of the negative muon SEU, we plan to perform more realistic muon transport and muonic X-ray simulations by considering the device board structure appropriately and compare the simulation and the present experimental result to validate the simulation code. By using the validated simulation code, we are going to investigate the mechanism of muon-induced SEU in detail, e.g., the relation among the stopping muon position, the species of the ions emitted via negative muon capture reaction on the atomic nuclei at the stopping position, and the SEU occurrence probability.

References

[1] B. D. Sierawski *et al.*, "Muon-induced single event upsets in deep-submicron technology," *IEEE Trans. Plasma Sci.*, vol. 57, no. 6, pp. 3273–3278, Dec. 2010.
[2] B. D. Sierawski *et al.*, "Effects of scaling on muon-induced soft errors," in *Proc. Int. Rel. Phys. Symp.*, Apr. 2011, pp. 3C.3.1–3C.3.6.
[3] B. D. Sierawski *et al.*, "Bias dependence of muon-induced single event upsets in 28 nm static random access memories," in *Proc. Int. Rel. Phys. Symp.*, Jun. 2014, pp. 2B.2.1–2B.2.5.
[4] N. Seifert, S. Jahinuzzaman, J. Velamala, and N. Patel, "Susceptibility of planar and 3D tri-gate technologies to muon-induced single event upsets," in *Proc. Int. Rel. Phys. Symp.*, Apr. 2015, pp. 2C.1.1–2C.1.6.
[5] G. Gasiot, D. Soussan, J. L. Autran, V. Malhere, and P. Roche, "Muons and thermal neutrons SEU characterization of 28 nm UTBB FD-SOI and bulk eSRAMs," in *Proc. Int. Rel. Phys. Symp.*, Apr. 2015, pp. 2C.2.1–2C.2.5.
[6] J. M. Trippe *et al.*, "Predicting muon-induced SEU rates for a 28-nm SRAM using protons and heavy ions to calibrate the sensitive volume model," *IEEE Trans. Nucl. Sci.*, vol. 65, no. 2, pp. 712–718, Feb. 2018.
[7] S. Serre *et al.*, "Effects of low energy muons on electronics: Physical insights and geant4 simulation," in *Proc. 13th Eur. Conf. Radiat. Effects Compon. Syst.*, Sep. 2012.
[8] S. Manabe *et al.*, "Negative and positive muon-induced single event upsets in 65-nm UTBB SOI SRAMs," *IEEE Trans. Nucl. Sci.*, vol. 65, no. 8, pp. 1742–1749, Aug. 2018.
[9] W. Liao *et al.*, "Measurement and mechanism investigation of negative and positive muon-induced upsets in 65-nm bulk SRAMs," *IEEE Trans. Nucl. Sci.*, vol. 65, no. 8, pp. 1734–1741, Aug. 2018.
[10] W. Liao, M. Hashimoto, S. Manabe, S.-I. Abe, and Y. Watanabe, "Similarity analysis on neutron- and negative muon-induced MCUs in 65-nm bulk SRAM," *IEEE Trans. Nucl. Sci.*, vol. 66, no. 7, pp. 1390–1397, Jul. 2019.
[11] S. Manabe, Y. Watanabe, W. Liao, M. Hashimoto, and S.-I. Abe, "Estimation of muon-induced SEU rates for 65-nm bulk and UTBB-SOI SRAMs," *IEEE Trans. Nucl. Sci.*, vol. 66, no. 7, pp. 1398–1403, Jul. 2019.
[12] W. Liao *et al.*, "Negative and positive muon-induced SEU cross sections in 28-nm and 65-nm planar bulk CMOS SRAMs," in *Proc. IEEE Int. Rel. Phys. Symp. (IRPS)*, Mar. 2019, pp. 1–9.
[13] S. E. Sobottka and E. L. Wills, "Energy spectrum of charged particles emitted following muon capture in Si^{28}," *Phys. Rev. Lett.*, vol. 20, no. 12, pp. 596–598, Jul. 2002.
[14] N. Seifert *et al.*, "Soft error rate improvements in 14-nm technology featuring second-generation 3D tri-gate transistors," *IEEE Trans. Nucl. Sci.*, vol. 62, no. 6, pp. 2570–2577, Dec. 2015.
[15] Y. Miyake *et al.*, "J-PARC muon source, MUSE," *Nucl. Instrum. Methods Phys. Res. A, Accel. Spectrom. Detect. Assoc. Equip.*, vol. 600, no. 1, pp. 22–24, Feb. 2009.
[16] Y. Miyake *et al.*, "J-PARC muon facility, MUSE," *J. Phys., Conf. Ser.*, vol. 225, Apr. 2010, Art. no. 012036.
[17] A. Sato *et al.*, "MuSIC, the world's highest intensity DC muon beam using a pion capture system," in *Proc. 2nd Int. Particle Accel. Conf. (IPAC)*, Sep. 2011, pp. 820–822.
[18] K. Terada *et al.*, "A new X-ray fluorescence spectroscopy for extraterrestrial materials using a muon beam," *Sci. Rep.*, vol. 4, May 2014, Art. no. 5072.
[19] T. Sato *et al.*, "Features of particle and heavy ion transport code system (PHITS) version 3.02," *J. Nucl. Sci. Technol.*, vol. 55, no. 6, pp. 684–690, Jun. 2018.